Journal of Applied Electrochemistry **30**: 617–624, 2000.

Copper corrosion at various pH values with and without the inhibitor

M. METIKOŠ-HUKOVIĆ, R. BABIĆ and I. PAIĆ
Department of Electrochemistry, Faculty of Chemical Engineering and Technology, University of Zagreb, Savska c. 16/1, PO Box 117, 10 000 Zagreb, Croatia

Received 7 May 1999; accepted in revised form 22 December 1999

Key words: adsorbtion isotherm, benzotriazole, copper, corrosion, finite diffusion impedance, inhibition

Abstract

The inhibitory action of BTAH on copper was investigated in 1 M sodium acetate solution in the pH range 4–10, using cyclic voltammetry and impedance spectroscopy. Cyclic voltammetry showed that the rearrangement of the surface oxide layer in the presence of BTAH is very fast in slightly alkaline solutions, while it is time- and concentration-dependent in neutral and slightly acidic solutions. The adsorption behaviour of BTAH on the electrode surface at $c(\text{BTAH}) \leq 0.5$ mM followed a Flory–Huggins adsorption isotherm with ΔG° ranging from -30.0 to -39.0 kJ mol^{-1}, depending on the pH. Impedance spectra were characterized by two time constants relating to the charge transfer and transport of copper ions through the oxide layer, the latter being the rate determining step. These enabled the determination of important properties of the adsorbed layer and the passivated film. The results indicate that the surface layer is of dielectric nature, and its protection increases with increasing inhibitor concentration and solution pH. The finite diffusion impedance was analysed using a diffusion factor B, and the values of the diffusion coefficient and concentration of copper species in the film were estimated.

List of symbols

A	surface area (cm^2)
B	diffusion factor (s$^{1/2}$)
B	constant of adsorption equilibrium (dm^3 mol^{-1})
c	concentration (mol dm^{-3})
C	capacity (F cm^{-2})
CPE	constant phase element
D	diffusion coefficient (cm^2 s^{-1})
d	thickness (nm)
E	potential (V)
F	faradaic constant (As mol^{-1})
f	frequency (Hz)
ΔG°	standard Gibbs energy change (kJ mol^{-1})
j	current density (A cm^{-2})
jω	complex variable for sinusoidal perturbations with $\omega = 2\pi f$
n	number of water molecules displaced by a molecule of inhibitor
n	CPE power
O	finite length diffusion element (Ω^{-1}/s$^{1/2}$)
Q	constant phase element (Ω^{-1}/s^n)
R	resistance (Ω cm^2)
R	gas constant (J K^{-1} mol^{-1})
Z	electrode impedance (Ω cm^2)
T	temperature (K)

Greek letters

θ	electrode coverage (%)
η	inhibition efficiency (%)
ω	angular velocity (rad s^{-1})
ε	dielectric constant
ε_o	vacuum permitivity
v	scan rate (mV s^{-1})
σ	Warburg coefficient (Ω cm^2 s$^{-1/2}$)

Sub/superscripts

ac	alternating current
corr	corrosion
ct	charge transfer
dc	direct current
f	film
i	inhibition
p	polarization

1. Introduction

Although copper is a relatively noble metal, it reacts easily in ordinary, oxygen-containing electrolytes [1]. For several decades the corrosion behaviour of copper in acidic, neutral and alkaline solutions has been explored [2]. In all cases the dissolution of copper was balanced by oxygen reduction. It was found that the corrosion rate of copper is influenced by the pH and has its lowest value in slightly alkaline solutions. In combination with electrochemical, ellipsometric and XPS surface analysis Brusic et al. [3] showed that the

stable oxides of copper can be formed reversibly in the pH range 8–12. At pH values below 7, the dissolution of copper becomes significant, especially below pH 5, where the formation of stable surface oxides is not possible. In a study of photoelectrochemical properties of corrosion products on copper, Di Quatro et al. [4] found that the growth of copper(I) oxide takes place in a range of pH values above 4. Feng et al. [2] found that the oxide film tends to dissolve in acidic solution, while the film thickness decreases rapidly with pH decreasing below 4. They have also found that copper dissolution is controlled mainly by diffusion in the solution phase, in solutions of pH below 4. With increasing pH, the formation of cubic Cu_2O oxide crystals was favoured; the oxide crystals became smaller, and the oxide films became thinner and more compact. This resulted in a change in dissolution control from mixed diffusion in oxide film, in solutions at pH 4 and pH 5, to diffusion in oxide film at pH 6 and above. In a pH 10 solution, a very thin, dense, and smooth Cu_2O layer formed on the electrode surface, resulting in spontaneous passivation [2], while at pH 12, a monoclinic CuO film formed, and the film thickness increased quickly with greater alkalinity. In sodium chloride solutions film stability was lower. Thus, Chen et al. [5] found that a surface film grew according to a linear law and had no protection in 0.5 M NaCl solution, even at pH 9.

However, in the presence of benzotriazole (BTAH), oxidation at the corrosion potential leads to the formation of a well-behaved film even in moderately acidic solutions. It is known that copper forms a cuprous benzotriazole complex, CuBTA, which is responsible for the corrosion inhibiting properties of BTAH [3, 6–8]. In sulphate solutions, a 0.01 M BTAH concentration inhibits corrosion of copper in the pH range 2 to 12, and is particularly effective in the pH range 4 to 10 [3]. This is consistent with the stability ranges for CuBTA in the E–pH diagram constructed by Tromans [9].

The CuBTA complex forms a chemisorbed layer at low coverage and a multilayer polymerized structure at larger film thickness [3, 7–13]. The details of the mechanism by which the film forms and protects the metal are the subject of much investigation and debate [3, 7, 14, 15].

The film growth can best be represented by a logarithmic law in the slightly alkaline and by a parabolic law in neutral and slightly acidic solutions [3]. Chen et al. [5] found that the film growth also depends on the concentration of BTAH, being parabolic at $c(\text{BTAH}) \leq 0.17$ mM, and logarithmic at $c(\text{BTAH}) \geq 0.17$ mM. The transition to either logarithmic or parabolic growth behaviour is an indication that ionic movement through the film has become the rate-determining step.

When considering the papers devoted to copper corrosion and inhibition, it can be seen that both the investigations in acetate solutions and those using low BTAH concentration, $c(\text{BTAH}) < 1$ mM, are very rare, especially in neutral or slightly acidic media. The aim of the present work is to investigate the inhibitory action of BTAH on copper, over a wide range of concentrations in acetate solution over the pH range 4 to 10, using potentiodynamic and impedance spectroscopy.

2. Experimental details

The working electrodes were prepared from pure Cu (99.999 wt.%). Samples for electrodes (15 mm dia. × 2 mm thick) were abraded with fine emery paper and polished with alumina powder down to 0.05 μm, and finally rinsed with distilled water and acetone. Prepared samples were embedded in a Teflon holder, so that an area of 1.00 cm^2 was exposed to the solution. A carbon rod and a saturated calomel electrode (SCE) served as counter electrode and reference electrode, respectively. All potentials were referred to the SCE scale. Measurements were performed in 1 M sodium acetate solution at pH values 4, 6, 8 and 10 with and without the addition of benzotriazole in the concentration range 0.01 to 5 mM. The pH values were adjusted with concentrated acetic acid or sodium hydroxide solution. Prior to each measurement the electrodes were subjected to cathodic pretreatment by holding them potentiostatically at −1.3 V for 60 s. The electrode was then subjected to a positive potential scan.

Impedance measurements were performed at E_{corr} with the a.c. voltage amplitude ±5 mV in the frequency range 30 mHz to 100 kHz. During the measurements, the solution was not stirred or deaerated. In fact, the preliminary investigation showed that the stirring did not influence the results of impedance measurements. Voltammetry and impedance measurements were carried out by a PAR EG&G potentiostat (model 273) and a PAR EG&G lock-in amplifier (model 5301A) with a personal computer.

3. Results and discussion

3.1. *Cyclic voltammetry*

Figure 1 represents the peak structure of the potentiodynamic polarization curves in the solutions of differnt pH. A broad region of anodic dissolution can be seen, and the anodic current densities are increased by one order of magnitude in the solutions at pH 4 and 6 compared to the solutions at pH 8 and 10. Generally, current peaks are well resolved except the anodic peaks at pH 6. Since two cathodic current peaks (the peaks C_1 and C_2) can be observed on cyclic voltammograms over the whole pH range investigated it can be assumed that they correspond at least to two anodic processes labelled by A_1 and A_2. Thus, the first anodic peak (A_1) has been assigned to the electroformation of a hydrous Cu_2O layer:

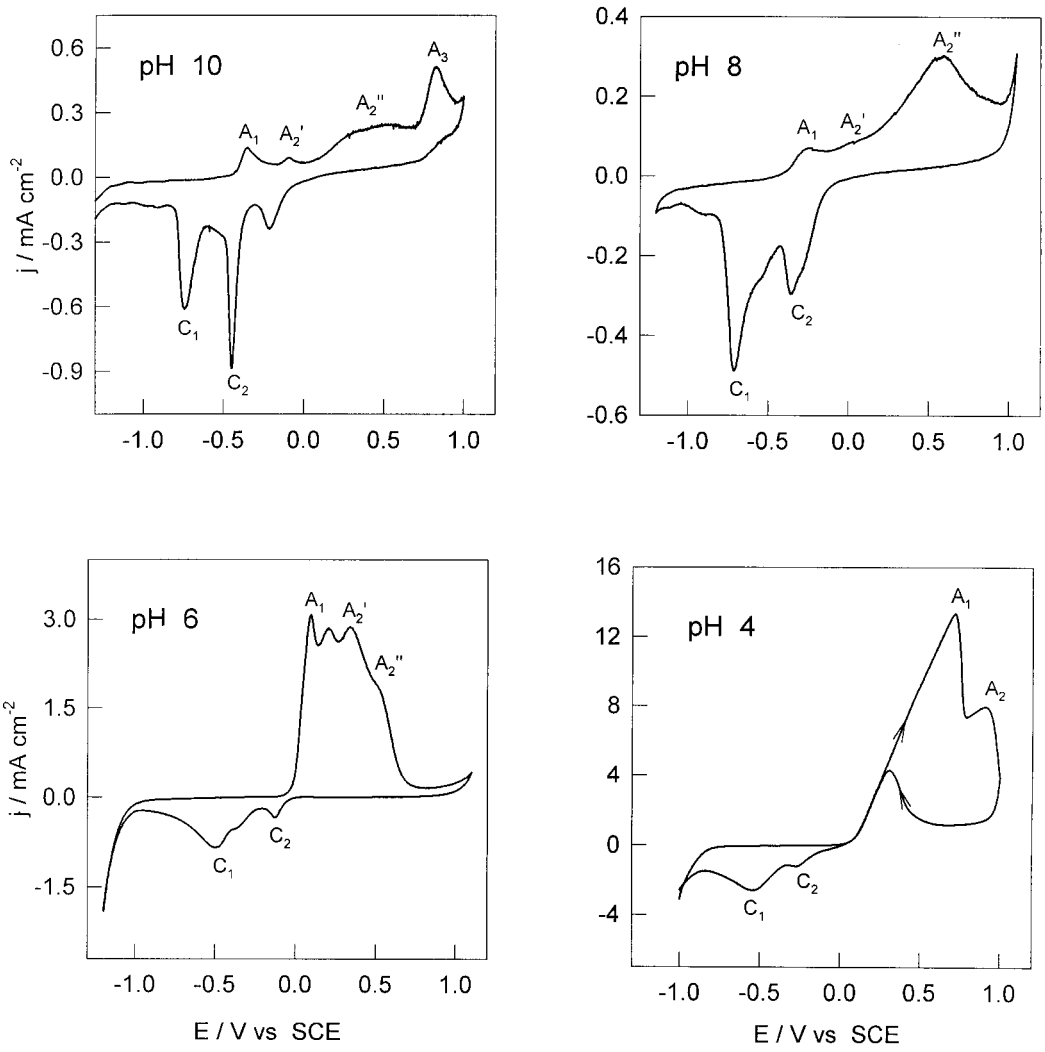

Fig. 1. Cyclic voltammograms on Cu in 1 M sodium acetate at specified pH values, ($v = 20$ mV s^{-1}).

$$2\,Cu + H_2O = Cu_2O + 2\,H^+ + 2\,e^-$$
$$E^\circ = 0.46\,V \text{ vs SHE}, \quad (1)$$

With increasing anodic potential the initially formed Cu_2O reacts with water yielding an outer layer [16]:

$$Cu_2O + (3-2x)H_2O = 2\,CuO_x(OH)_{2-2x} + 2\,H^+ + 2\,e^- \quad (2)$$

responsible for the second anodic current peak (A_2), as well as the duplex structure of the passive layer [16–23]. According to Sato et al. [16] the value of x in Equation 2 is changeable in the range 0 to 1, but with increasing anodic potential its value also increases. In many cases the current peak A_2 is split into two current peaks that are usually assigned to the electroformation of CuO and hydrated $Cu(OH)_2$ as follows from Equation 2.

The third anodic current peak (A_3) at pH 10 is thought to be due to the formation of Cu_2O_3 [18, 24] before oxygen evolution. Evidence for the formation of this oxide species is gained from the corresponding cathodic sweep, where the first cathodic current maximum (C_3) indicates the reduction of a metastable copper species from a higher to a lower oxidation state. The other two cathodic current maxima (C_2,C_1) observed at pH 10, as well as both cathodic current peaks observed at the other pH values, correspond to the reduction of a duplex oxide film on the electrode surface. The cathodic reduction of the outer layer to Cu_2O proceeds with a backward reaction of Equation 2, starting from the outer–inner layer interface towards the outer layer–solution interface. Finally, the last cathodic current peak (C_1) corresponds to the reduction of the total Cu_2O film to metallic copper involving the inner layer according to the backward reaction of Equation 1.

In Figure 2, the cyclic voltammograms obtained on copper in a pure sodium acetate solution and in the presence of 0.5 M BTAH at pH 10 are presented. It can be seen that the anodic current density and anodic peak resolution are significantly decreased in the presence of BTAH. As far as the cathodic range is concerned, a decrease in current density can also be observed, although the main difference is that the peaks' position

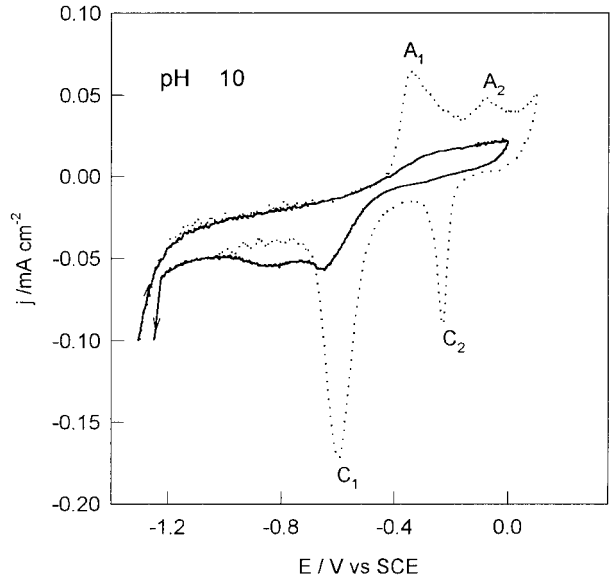

Fig. 2. Cyclic voltammograms on Cu in 1 M sodium acetate, pH 10, without (-----) and with the presence of 0.5 M BTAH (——), ($v = 10$ mV s^{-1}).

is shifted for about 400 mV towards more negative potential values. The same behaviour is observed at pH 8. This could indicate that the interaction of copper oxide with BTAH and the rearrangement of the film itself are very fast in slightly alkaline solutions. Very similar behaviour was also observed by Sutter et al. [25] in 0.1 M sodium acetate (pH 8.7). In slightly acidic solutions, the cathodic peaks were shifted towards more negative potential values only when the electrodes were immersed in a solution containing BTAH for a longer period of time [12, 26]. It seems that the same potential shift observed in slightly alkaline and slightly acidic acetate solutions indicates almost identical composition of the surface layers, that is, the formation of a complex (CuBTA) compound. The reason why the complex formation and film rearrangement are pH dependent probably lies in the fact that BTAH acts as a very weak acid ($pK_a = 8.2$ [27]), and that its extent of ionization depends on the solution pH (Table 1). In 0.5 M BTAH, at pH 6, the concentration of free BTA^- ions amounts to only 6.31×10^{-3} M (BTAH is approximately 1.26% ionized), while at 10 the ionization is 100%. In slightly acidic solutions, the initially adsorbed molecules of BTAH on copper surface have to ionize prior to the complex formation and their ionization is obviously a slow process. In slightly alkaline solutions, the concentration of free BTA^- ions is relatively high. After being absorbed, they react immediately with copper oxide yielding a complex (CuBTA) compound that is responsible for a potential shift of the cathodic current peaks.

Table 1. Percentage of BTAH ionization as a function of pH of 1 M sodium acetate

pH	4.0	6.0	8.0	10.0
Ionization/%	0.0126	1.26	63.0	100

The values of electrode coverage, θ, in dependence of of the inhibitor concentration were calculated at 0.1 V using the equation $\theta = 100[1 - (j_a)_i/(j_a)_o]$, where subscripts o and i denote the unhibited and inhibited electrolyte, respectively. It is found that the data for the electrode coverage corresponding to the BTAH concentration from 0.01 to 0.1 mM, can be well fitted to the Flory–Huggins adsorption isotherm:

$$\frac{\theta}{(1-\theta)^n}\frac{[\theta + n(1-\theta)]^{n-1}}{n^n} = c_i K = \frac{c_i}{55.5}\exp\left(\frac{-\Delta G^\circ}{RT}\right) \quad (3)$$

where K is the adsorption equilibrium constant, c_i is the inhibitor concentration, n is the number of water molecules displaced by a molecule of inhibitor, and ΔG° is the Gibbs energy change. The values of Gibbs energy change are presented in Table 2. In all cases, they indicate a strong adsorption of BTAH on the electrode surface, although little stronger in slightly acidic than in alkaline solutions. Similar results for ΔG° values were obtained by Fox and coworkers [28] for Cu in 0.2 M NH_4Cl solution having BTAH concentration less than 10^{-3} M.

3.2. *Impedance measurements*

Impedance measurements on the Cu electrode in 1 M sodium acetate (pH 4, 6, 8 and 10), alone and in the presence of various concentrations of inhibitor, were performed at the open-circuit potential. The influence of BTAH concentration on impedance spectra of copper at pH 4 is presented in Figure 3 in the form of a Bode plot. The similar behaviour is observed at the other pH values. The Figure shows that the $\log|Z|$ against $\log f$ curves exhibit three distinctive segments. In the higher frequency region, the $\log|Z|$ values are low and tend to become constant, while phase angle values fall rapidly towards 0°. This response is typical for resistive behaviour and corresponds to solution resistance. In the medium frequency region, a linear relationship can be observed between $\log|Z|$ against $\log f$, with the slope close to -1 and the phase angle approaching $-90\,°$. This is a characteristic response for capacitive behaviour. In the low-frequency region, the resistive behaviour of the electrode increases, but the region where $\log|Z|$ does not depend on $\log f$ (i.e. the d.c. limit) is not completely reached. All measurements have shown that both the capacitive and low frequency resistive regions of the impedance shift to higher values of impedance with increasing pH and concentration of BTAH, especially

Table 2. Gibbs energy change of adsorption of BTAH on a copper electrode and the constant n in the Flory–Huggins isotherm as a function of pH of 1 M sodium acetate

pH	4.0	6	8	10
ΔG°/kJ mol^{-1}	−37.54	−39.00	−31.06	−30.04
n	0.5	1.5	0.8	1.2

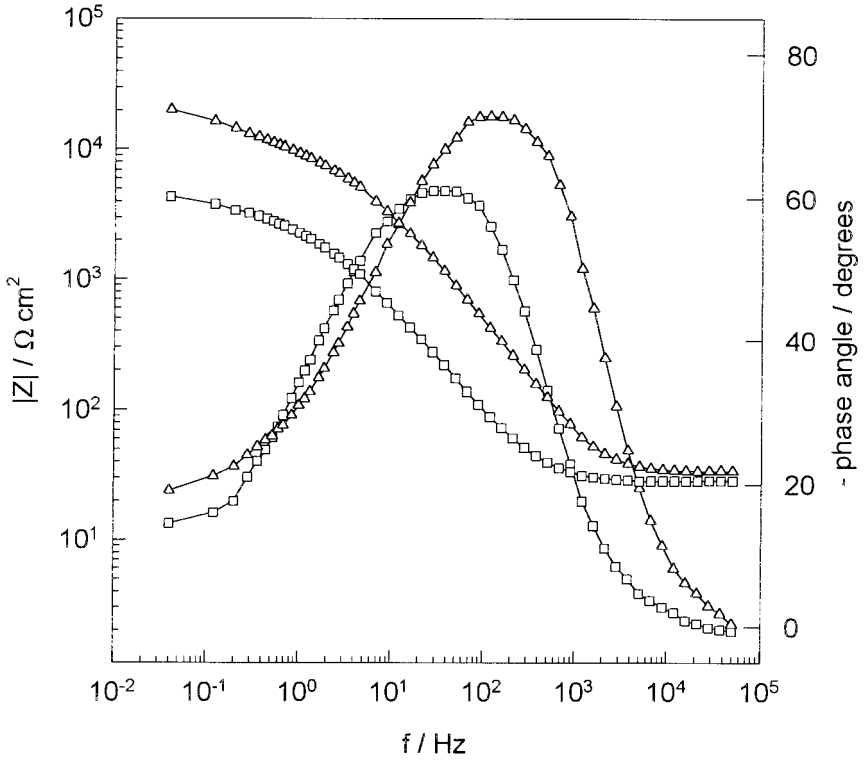

Fig. 3. Bode plots for Cu in 1 M sodium acetate, pH 4, in the presence of 0.01 mM (□) and 0.5 mM (Δ) of BTAH.

for concentrations higher than 0.5 mM. A closer inspection of the medium and low frequency ranges shows that the mass transport occurring through the phase layer must be taken into account and that the corresponding equivalent circuit of the system must contain more than one time constant. The equivalent circuit proposed to fit the experimental data is presented in Figure 4. It consists of solution resistance R_Ω in a serial connection with two time constants.

The first time constant, R_1C_1, in the high frequency region is proposed to be a result of a fast charge transfer process of copper dissolution; R_1 being the charge transfer resistance, R_{ct}, and C_1 being the double layer capacitance. Since the electrochemical systems show various types of inhomogeneities [29], they can be better described by a transfer function with constant phase elements (CPE). Its impedance is given by

$$Z_1 = \frac{R_1}{1 + R_1 Q(\mathrm{j}\omega)^n} \tag{4}$$

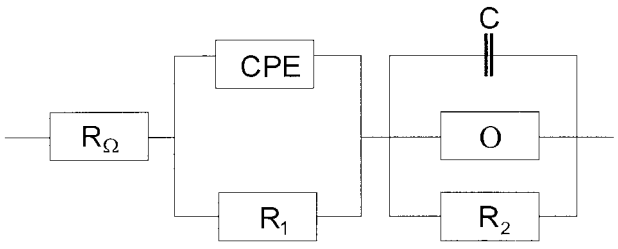

Fig. 4. Equivalent electrical circuit used to fit the impedance spectra.

where j is the imaginary number ($\mathrm{j}^2 = -1$), Q is the frequency-independent real constant, ω is the angular frequency, n is the CPE power, $n = \alpha/(\pi/2)$, and α is the phase angle of the CPE. The factor n is an adjustable parameter that usually lies between 0.5 and 1 [30]. The CPE only describes an ideal capacitor when $n = 1$. Otherwise, for $0.5 < n < 1$ the CPE describes a distribution of dielectric relaxation times in frequency space. The CPE element was introduced formally only for fitting impedance data [31].

The second time constant in the low impedance region, given by

$$Z_2 = \frac{R_2}{1 + R_2\mathrm{j}\omega C + R_2 O(\mathrm{j}\omega)^{0.5}\coth[B(\mathrm{j}\omega)^{0.5}]} \tag{5}$$

results from mass transport through the oxide film; C is the capacitance of the surface film, R_2 the surface layer resistance, B the diffusion factor and O is the finite length diffusion element. The total impedance Z of the electrochemical system was found by adding the resistance of the electrolyte, R_Ω, to the impedance of the electrochemical interface:

$$Z_{\text{total}} = R_\Omega + \frac{R_1}{1 + R_1 Q(\mathrm{j}\omega)^n} + \frac{R_2}{1 + R_2\mathrm{j}\omega C + R_2 O(\mathrm{j}\omega)^{0.5}\coth[B(\mathrm{j}\omega)^{0.5}]} \tag{6}$$

The quantitative analysis of the experimental impedance data was performed by a nonlinear least squares minimization method developed by Boukamp [31]. This

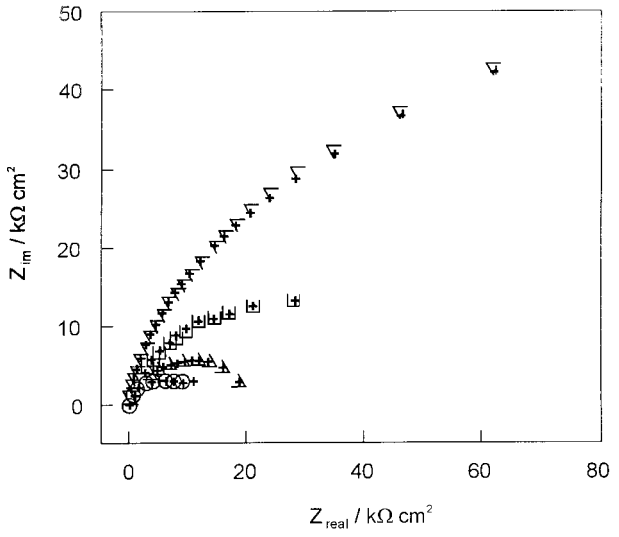

Fig. 5. Measured (symbols) and simulated (+) spectra for Cu in 0.5 mM of BTAH at (○) pH 4, (Δ) pH 6, (□) pH 8 and (▽) pH 10.

method simultaneously fits imaginary and the real part of the impedance data and provides uncertainty estimates for all estimated parameters, as well as allowing one to fit complete transfer function having several parameters. The quality of the fit is illustrated in Figure 5, where impedance data obtained at the inhibitor concentration equal to 0.5 mM, and at pH values 4, 6, 8 and 10 are shown in Nyquist plot together with calculated curves using the fit parameters extracted.

The fit parameters obtained at different pH values and for various concentrations of BTAH were extracted and analysed. For an illustration, the fit parameters obtained for copper inhibition at pH 4 and pH 10 are presented in Tables 3 and 4.

In real 3D inhomogeneous systems [32], as the investigated Cu/surface layer/electrolyte solution, because of the time dependent formation of the porous or compact barrier layer, the kinetic resistance is a complicated function determined by charge transfer, mass transport and chemical reaction rate [33].

The total resistance of the copper/electrolyte interphase, R, includes R_1 and R_2 values and a real value of the finite diffusion at $\omega \to 0$ ($Z_w = B/O$). In Figure 6, the total resistance is presented as a function of pH and concentration of BTAH. In all cases R increases with increasing inhibitor concentration and pH. The total resistance of the system can be used to calculate the inhibiting efficiency, $\eta_{ac} = (R_i - R_o)/R_i$, where R_i and R_o are resistances with and without the inhibitor, respectively. Since the oxide layer on copper has weaker protecting efficiency in acidic solutions, the inhibiting efficiency of BTAH is very high in those solutions. At pH 4, almost 90% inhibiting efficiency of BTAH is reached at the inhibitor concentration of 0.5 mM.

Tables 3 and 4 show that the capacitance of copper electrode decreases with increasing BTAH concentration. The decrease in capacitance with increasing inhibitor concentration is attributed to the formation of a protective film on the electrode surface. At higher inhibitor concentration, the slope of the $\log|Z|$ against $\log f$ was close to -1 and the phase shift was close to $-90\,^\circ$, indicating the behaviour of an ideal capacitor. Assuming a parallel plate condenser behaviour, a rough estimate of the thickness values, d, for the films formed at various conditions could be made by $d = \varepsilon\ \varepsilon_o A/C$, where ε is the dielectric constant of the surface film, ε_o is the dielectric constant of free space, A is the exposed area of the test electrode and d is the thickness of the coating. For a capacitance of 1.87 μF cm^{-2} (pH 10.0 and c(BTAH) = 5 mM), $\varepsilon = 19.9$ [34] and $\varepsilon_o = 8.85 \times 10^{-14}$ F cm^{-1}, the value of d is about 9.40 nm. The obtained value seems quite reasonable in comparison with those obtained in slightly alkaline solutions [5, 7, 10].

Table 3. Impedance parameters for Cu in 1 M acetate solution, pH 4, in the presence of BTAH at various concentrations

c (BTAH) /mmol dm^3	R_1 /kΩ cm^2	$10^6 \times Q$ /Ω^{-1} s^n cm^{-2}	n	$10^6 \times C$ /F cm^{-2}	R_2 /kΩ cm^2	$10^5 \times O$ /Ω^{-1} s$^{0.5}$ cm^{-2}	B /s$^{0.5}$	R /kΩ cm^2	η /%
0	0.523	106.50	0.89	11.51	2.40	15.70	3.37	2.68	
0.01	1.78	80.60	0.85	29.30	3.80	31.00	6.10	4.96	45.9
0.1	3.30	19.40	0.90	7.65	12.00	8.65	6.55	13.66	80.38
0.5	3.30	12.96	0.94	3.66	25.05	4.73	6.36	24.42	89.0
1	2.68	51.60	1.00	2.64	39.94	7.36	8.82	32.64	91.8
5	1.44	63.46	1.00	1.55	68.59	5.31	17.00	57.93	95.4

Table 4. Impedance parameters for Cu in 1 M acetate solution, pH 10, in the presence of BTAH at various concentrations

c (BTAH) /mmol dm^{-3}	R_1 /kΩ cm^2	$10^6 \times Q$ /Ω^{-1} s^n cm^{-2}	n	$10^6 \times C$ /F cm^{-2}	R_2 /kΩ cm^2	$10^5 \times O$ /Ω^{-1} s$^{0.5}$ cm^{-2}	B /s$^{0.5}$	R /kΩ cm^2	η /%
0	0.79	210.6	0.81	8.18	48.49	7.20	4.04	26.80	
0.01	9.74	42.0	0.89	5.58	141.90	4.33	3.24	58.73	54.3
0.05	13.36	23.7	0.89	4.28	99.28	2.65	4.44	75.70	64.6
0.1	6.39	46.4	0.88	4.26	113.60	2.34	4.00	74.64	64.1
0.5	7.41	40.7	0.88	4.45	199.20	1.48	4.00	122.09	78.0
1	43.37	20.8	0.86	4.05	208.00	2.87	4.10	128.06	79.0
5	66.22	8.5	0.89	1.87	340.40	6.10	5.00	132.28	79.7

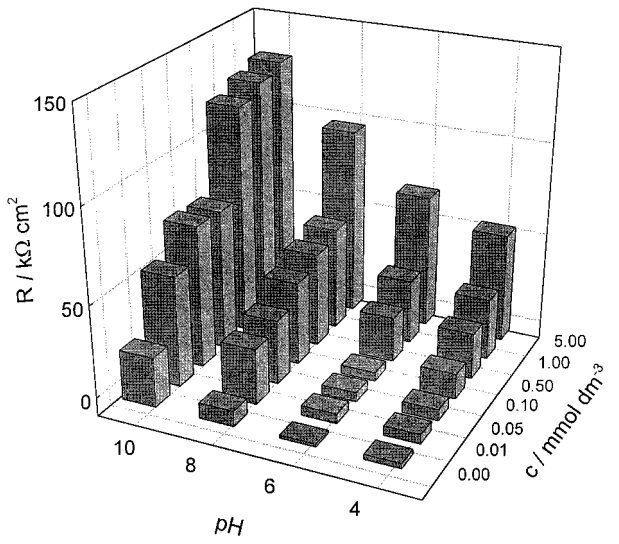

Fig. 6. 3D plot representing the influence of pH and c(BTAH) on the total resistance of a Cu electrode.

Although the calculated thickness value seems quite reasonable, there is a problem concerning the ε value. The results show that the capacity values at a certain inhibitor concentration lie in a very narrow range over the pH range investigated (1.5–1.9 μF cm^{-2} at c(BTAH) = 5 mM). As the difference in film resistance is much larger (70–400 kΩ cm^2 in the pH range 4–10), the film structure is obviously different, and a change in the dielectric constant could be expected.

Since the Warburg impedance was assessed as a film diffusion process where the diffusion layer thickness, d, can replace the thickness of the film [35] through which the diffusion takes place, it follows that:

$$B = d\left(\frac{1}{D_f}\right)^{0.5} \tag{7}$$

where D_f is the film diffusion coefficient. B data presented in Tables 3 and 4 make possible the calculation of the film diffusion coefficient. Thus, for $d = 9.40$ nm (pH 10, c(BTAH) = 5 mM), and for $B = 4.56$, a value of $D_f = 4.0 \times 10^{-14}$ cm^2 s^{-1} is obtained, which is in a good agreement with D_f usually reported for diffusion in solid films [36, 37].

The value of D_f was used to calculate the concentration, c_f, of the diffusing copper species in the film according to the equation:

$$\sigma = \frac{RT}{\sqrt{2} \times n^2F^2} \times \frac{1}{c_f\sqrt{D_f}} \tag{8}$$

where Warburg coefficient, σ is equal $1\sqrt{2}O$.

The value for the concentration of mobile species was found to be $c_f = 8.0 \times 10^{-6}$ mol cm^{-3}. Since the diffusion appears to operate within the film, Fick's law of diffusion may be written as

$$j_p = \frac{nFc_fD_f}{d} \tag{9}$$

where j_p is the passivating current flowing through the film. The value of the diffusion current was calculated to be $j_p = 3 \times 10^{-2}$ μA cm^{-2}, which seems quite plausible. Corrosion currents of the same order of magnitude for copper inhibited by BTAH in slightly alkaline solutions were reported [3].

4. Conclusion

The inhibitory action of BTAH on copper was investigated in 1 M sodium acetate solution in the pH range 4–10, using cyclic voltammetry and impedance spectroscopy techniques. Cyclic voltammetry showed that copper passivation corresponds to the electroformation of a barrier Cu_2O layer followed by a hydrous and more soluble CuO layer. The addition of BTAH decreased the anodic current density and modified the surface film. In slightly alkaline solutions, the film rearrangement was almost instantaneous, due to almost complete dissociation of BTAH, resulting in the shift of the cathodic current peak toward more negative potentials. In neutral and slightly acidic solutions, the film rearrangement was time dependent. At solution concentrations of BTAH less than 0.5 mM, the inhibitor adsorption followed a Flory–Huggins adsorption isotherm with ΔG° ranging from -30.0 to -39.0 kJ mol^{-1}, depending on the pH.

Impedance spectra obtained in a wide range of inhibitor concentrations and in the pH range 4–10 were determined by two time constants, the first one relating to the charge transfer process and the second one including the mass transport of copper ions through the oxide film. The analysis of impedance spectra showed high inhibiting efficiency of BTAH even at relatively low concentration (close to 90% at c(BTAH) = 0.5 mM). It also indicated that film thickness could be monitored *in situ* by impedance measurements. At 5 mM BTAH and pH 10, a 10 nm film thickness was observed, while the diffusion coefficient and concentration of metallic species in the film were of the order of 10^{-14} cm^2 s^{-1} and 10^{-6} mol cm^{-3}, respectively.

Acknowledgement

This work was supported by the Ministry of Science of the Republic of Croatia through Project 125011.

References

1. M. Pourbaix, '*Atlas of Electrochemical Equilibria in Aqueous Solutions*' (Pergamon Press, New York, 1966).
2. Y. Feng, K.-S. Siow, W.-K. Teo, K.-L. Tan and A.-K. Hseih, *Corrosion* **53** (1997) 389.
3. V. Brusic, M.A. Frisch, B.N. Eldridge, F.P. Novak, F.B. Kaufman, B.M. Rush and G.S. Frankel, *J. Electrochem. Soc.* **138** (1991) 2253.
4. F. Di Quarto, S. Piazza and C. Sunseri, *Electrochim. Acta* **30** (1985) 315.

5. J.-H. Chen, Z.-C. Lin, S. Chen, L.-H. Nie and S.-Z. Yao, *Electrochim. Acta* **43** (1998) 265.
6. J.B. Cotton and I.R. Scholes, *Br. Corros. J.* **2** (1967) 1.
7. G.W. Poling, *Corros. Sci.* **10** (1970) 359.
8. T. Notoya and G.W. Poling, *Corrosion* **32** (1976) 216.
9. D. Tromans, *J. Electrochem. Soc.* **145** (1998) L42.
10. F. Mansfeld and T. Smith, *Corrosion* **29** (1973) 105.
11. M.R. Vogt, W. Polewsa, O.M. Magnussen and R.J. Behm, *J. Electrochem. Soc.* **144** (1997) L113.
12. M. Metikos-Hukovic, R. Babic and A. Marinovic, *J. Electrochem. Soc.* **145** (1998) 4045.
13. R. Babic, M. Metikos-Hukovic and M. Loncar, *Electrochim. Acta* **44** (1999) 2413.
14. D. Tromans and R.-H. Sun, *J. Electrochem. Soc.* **138** (1991) 3235.
15. A.D. Modestov, G.D. Zhou, Y.P. Wu, T. Notoya and D.P. Schweinsberg, *Corros. Sci.* **36** (1994) 1931.
16. M. Seo, X.C. Jiang and N. Sato, *Werkstoff. u. Korr.* **39** (1988) 583.
17. H.Y.H. Chan, C.G. Takoudis and M.J. Weaver, *J. Phys. Chem.* B **103** (1999) 357.
18. S.T. Mayer and R.H. Muller, *J. Electrochem. Soc.* **139** (1992) 426.
19. W. Kautek and J.G. Gordon II, *J. Electrochem. Soc.* **137** (1990) 2672.
20. H.D. Speckmann, M.M. Lohrengel, J.W. Schultze and H.H. Strehblow, *Ber. Bunsenges. Phys. Chem.* **89** (1985) 392.
21. L.D. Burke, M.J.G. Ahern and T.G. Ryan, *J. Electrochem. Soc.* **137** (1990) 553.
22. C.-H. Pyun, S.-M. Park, *J. Electrochem. Soc.* **133** (1986) 2024.
23. A. Aruchamy and Fujishima, *J. Electroanal. Chem.* **266** (1989) 397.
24. S.M. A.-E. Haleem and B.G. Ateya, *J. Electroanal. Chem.* **117** (1981) 309.
25. E.M.M. Sutter, C. Fiaud and D. Lincot, *Electrochim. Acta* **38** (1993) 1471.
26. F. Ammeloot, C. Fiaud and E.M.M. Sutter, *Electrochim. Acta* **42** (1997) 3565.
27. D.D. Perrin, 'Dissociation Constants of Organic Bases in Aqueous Solutions' (Butterworths, London, 1965).
28. P.G. Fox, G. Lewis and P.J. Boden, *Corros. Sci.* **19** (1979) 457.
29. K. Juttner, J.W. Lorentz, M.W. Kending and F. Mansfeld, *J. Electrochem. Soc.* **135** (1988) 332.
30. U. Rammelt and G. Reinhard, *Electrochim. Acta* **35** (1990) 1045.
31. B.A. Boukamp, 'Equivalent Circuit', International Report CT 89/214/128, University of Twente.
32. K. Jutner, *Electrochim. Acta* **35** (1990) 1501.
33. E. Kalman, B. Varhegyi, I. Bako, I. Felhosi, F.H. Karman and A. Shaban, *J. Electrochem. Soc.* **141** (1994) 3357.
34. F. El-Taib Heakal, S. Haruyama, *Corros. Sci.* **20** (1980) 887.
35. J.L. Dawson and D.G. John, *Electroanal. Chem.* **110** (1980) 37.
36. M. Bojinov and D. Pavlov, *J. Electroanal. Chem.* **315** (1991) 201.
37. L.M. Gassa, H.T. Mishima, B.A. Lopez de Mishima and J.R. Vilche, *Electrochim. Acta* **42** (1997) 1717.